The following supplement accompanies the article:

Environmental conditions are poor predictors of immature white shark *Carcharodon carcharias* occurrences on coastal beaches of eastern Australia

Julia L.Y. Spaet[1, 2*], Andrea Manica[1], Craig P. Brand[3], Christopher Gallen[4], Paul A. Butcher[2,3]

[1]Evolutionary Ecology Group, Department of Zoology, University of Cambridge, Cambridge CB2 3EJ, UK
[2] Southern Cross University, Coffs Harbour, New South Wales 2450, Australia
[3]Fisheries NSW, NSW Department of Primary Industries, National Marine Science Centre, Coffs Harbour, New South Wales 2450, Australia
[4]Fisheries NSW, NSW Department of Primary Industries, Port Stephens Fisheries Institute, Nelson Bay, New South Wales 2315, Australia

* Corresponding author: jlys3@cam.ac.uk

Table S1. Number of sharks caught, detected and total number of detections by each of the four capture methods employed.

Method of capture	Number of sharks tagged	Number of sharks detected	Total number of detections (after hourly binning)
SMART drumlines	406	328	7678
Baited hooks	14	3	14
Surface-buoyed setlines	7	6	53
Bather protection nets	17	2	73

Text S1: Range testing and receiver performance

Methods

Between 15 July 2019 and 30 November 2019, 10 precision fixed delay transmitters (V16-6L InnovaSea, Marine Systems Canada, Inc., Halifax, Nova Scotia) with a frequency of 69 kHz and 10 min fixed delay transmission intervals were placed at distances of 100 m and 200 m offshore from VR4G receiver units at Evans Head, South West Rocks, Port Macquarie, Forster and Hawks Nest (Table S2). Towards the end of the range test period, four additional transmitters were placed at a distance of 500 m at all range test locations except Forster (Table S2). The 5 selected range test locations were considered array-representative and were chosen for logistical reasons. Transmitters embedded in PVC casings were attached in a vertical position at the 2 m point of a 3 m (10 mm diameter) rope between a 150 mm diameter buoy and a 23-kg iron bar on the sea bed. To monitor changes in detection performance over the course of the study period and to record ambient water temperature, each receiver was also equipped with a stationary reference (sentinel) tag (V16T-4x, InnovaSea, Marine Systems Canada, Inc., Halifax, Nova Scotia), programmed to transmit an acoustic code every 4 h throughout the entire study period. Sentinel tags were embedded in polyvinyl chloride tubes with 8 mm holes drilled to allow water flow and attached either to the riser rope or the base of the VR4G leg, at about 1–2 m from the hydrophone and 2–4 m below the sea surface. Assuming a 100% detection rate (number of detections recorded by a receiver divided by the known number of transmissions emitted), 6,564 total transmissions per tag were expected over the 1,094 day study period.

To assess the effect of the same 5 variables investigated in the main study (i.e. time of day, water temperature, tidal height, swell height and lunar phase) on detection efficiency (the probability of a transmission from a tag being successfully detected by a receiver), we binned the range test detection data collected by hour for each receiver–tag combination and linked the resulting data to the selected variables for the same time period. We then used the same generalized additive model (GAM) approach as described in the main document under *2.3.1*. We ran all possible combinations of explanatory variables alongside

the null model and calculated AICc values using the 'dredge' function in the R package MuMIn (Bartoń 2019). Candidate models were ranked according to AICc and weight. We then individually assessed the importance of variables based on the proportion of deviance explained. For each variable, we calculated the predictive deviance uniquely explained by that variable by subtracting the deviance of the model excluding that variable from the full model deviance. For each model, we included location and distance as additive fixed effects to correct for pseudo-replication and account for unknown differences inherent to each location that are otherwise unaccounted for in our analysis.

To define variability in detection rate over time, the number of detections per day by location and distance was assessed and plotted over the total range test period. In addition, for each sentinel tag, the number of detections per hour by location was assessed over the total study period to define any diel differences in detection patterns. Each detection was assigned to 1 of 24 bins based upon the hour of the detection. Under a hypothesized equal distribution of detections over a 24 h period, Chi-square goodness-of-fit tests were performed to determine whether the observed proportion of detections differed significantly from an expected even distribution.

Results

The acoustic environment at all receiver locations was highly variable over spatial and temporal scales (Fig. S1). Detection efficiency of all receivers decreased with distance; all but the receiver at Port Macquarie also showed a decrease in detection efficiency over time (Fig. S1). The final GAM chosen through the model selection process retained all explanatory variables and explained 21.54% of the variation in detections (Table S3). The GAM revealed a highly significant ($p < 0.001$) negative effect of increasing swell height on detection efficiency (Fig. S2). Receivers performed best at temperatures between 18ºC to 19ºC. At higher temperatures graphical GAM output showed a highly significant ($p < 0.001$) negative effect of increasing temperature on detection efficiency (Fig. S2). Time of day, tidal height and lunar phase exhibited a highly significant ($p< 0.001$) positive effect, with increasing detection efficiency with time of day (from night to day), tidal height and lunar phase (from new to full moon) (Fig. S2). Unique deviance explained by the five variables tested ranged from 0.22% (lunar phase) to 5.14% (temperature) (Table S4). Distance between range test transmitters and receivers explained 8.49% of the observed variability, while receiver location accounted for 4.9% (Table S4).

Total detection rates of sentinel tags by VR4G receivers ranged from 72% (Byron Bay) to 91% Forster (Fig. S3). VR4G receivers at Kingscliff and Lennox Head recorded significantly more sentinel detections during daytime than during night (chi-square tests: p=0.01 and

p=0.001, respectively), for all other receivers detections were distributed evenly across hourly bins (p>0.5) (Fig. S3).

Discussion

We observed considerable spatial and temporal variability in the detection efficiency of range test transmitters and all environmental factors tested were found to alter signal attenuation across all five range test receiver locations. Water temperature was the dominant driver of detection variability, with GAM response curves showing an exponential decrease in detection rates at temperatures above 19ºC across all range test receiver locations. While a negative relationship between temperature and detection efficiency has been reported in several studies (How & de Lestang 2012, e.g. Cagua et al. 2013, Mathies et al. 2014, Huveneers et al. 2016), this is contrary to acoustic theory, where signal strength and hence detection rates increase in higher water temperatures through reduced absorption at the signal frequency (Winter 1996, Medwin & Clay 1997). Two possible phenomena might explain the observed patterns: (1) Periods of increased temperature over relatively shallow sandy bottoms may have caused a thermocline to establish (How & de Lestang 2012). Thermoclines and stratification can cause sound signals to change speed or refract resulting in reduced detection efficiency (Voegeli & Pincock 1996, Heupel et al. 2006, Mathies et al. 2014) or reductions in acoustic range (Singh et al. 2009, Huveneers et al. 2016). (2) Warmer temperatures may have stimulated increased activity in ectothermic organisms, such as snapping shrimps (Radford et al. 2008, Payne et al. 2010, Cagua et al. 2013), and hence biological noise in the tag's frequency range.

Biological noise is likely also responsible for (a) the strong diurnal pattern in detections with smaller detection efficiency at night, and (b) the significant differences corresponding to the lunar phase. Diel and lunar patterns in biological noise, with more noise occurring at night (Payne et al. 2010, How & de Lestang 2012, Cagua et al. 2013) and around the new moon (Radford et al. 2008), have been directly recorded in various marine ecosystems. These observations coincide with evidence of decreasing acoustic detections at night (Payne et al. 2010, How & de Lestang 2012, Cagua et al. 2013) and around the new moon (How & de Lestang 2012, Cagua et al. 2013). The strong negative influence of swell height on receiver performance was expected and is likely attributed to an increase in noise from breaking waves (Gjelland & Hedger 2013). We were unable to clearly define the sources of noise that induced variability in detection efficiency. However, long-term noise level measurements around all 21 receivers deployed are currently being conducted, allowing future studies to directly correlate receiver-specific detection efficiency with receiver-specific ambient noise levels.

An increase of biofouling organisms attached to receivers has also been shown to affect detection rate over time (Heupel et al. 2008). In the present study, receivers were periodically cleaned. Receiver performance was investigated after each cleaning event to check for spikes in detection rate, which would indicate a negative effect of biofouling on receiver performance. Although, biofouling was visually apparent on receivers, a positive increase in detection efficiency after cleaning events was not visible. Biofouling hence does not seem to play a large role in the observed decrease in detection efficiency over time.

Although the variables tested explained some of the observed variability, much of it (~80%) remains unexplained, highlighting the complex nature of acoustics in natural systems. Besides environmental variables, sediment characteristics, topography, bathymetry, substrate, obstructions, mooring designs, tag transmission characteristics, transmitter attachments and receiver configuration have been shown to influence detection efficiency (Clements et al. 2005, Heupel et al. 2006, Simpfendorfer et al. 2008, Cagua et al. 2013, Dance et al. 2016). While some of these factors can be minimized through careful planning or adjustments of the original study design, the relationships between detection efficiency and the five environmental variables examined here cannot be controlled. For future studies, we hence consider the incorporation of *in situ* measures of system performance throughout the course of the study, followed by retrospective analyses of array performance as the best defence against biased study conclusions. The suggested approach will allow to correct for variability of all measured environmental variables by integrating measures of receiver-specific detection efficiency directly into statistical analyses (e.g. Gjelland & Hedger 2013, Winton et al. 2018).

Literature cited

Barton K (2020) Package 'MuMIn': Multi-Model Inference. R Packag version 1.43.17. https://CRAN.R-project.org/package=MuMIn

Cagua EF, Berumen ML, Tyler EHM (2013) Topography and biological noise determine acoustic detectability on coral reefs. Coral Reefs 32:1123–1134.

Clements S, Jepsen D, Karnowski M, Schreck CB (2005) Optimization of an acoustic telemetry array for detecting transmitter-implanted fish. North Am J Fish Manag 25:429–436.

Dance MA, Moulton DL, Furey NB, Rooker JR (2016) Does transmitter placement or species affect detection efficiency of tagged animals in biotelemetry research? Fish Res 183:80–85.

Gjelland KØ, Hedger RD (2013) Environmental influence on transmitter detection probability in biotelemetry: developing a general model of acoustic transmission. Methods Ecol Evol 4:665–674.

Heupel MR, Reiss KL, Yeiser BG, Simpfendorfer CA (2008) Effects of biofouling on performance of moored data logging acoustic receivers. Limnol Oceanogr Methods 6:327–335.

Heupel MR, Semmens JM, Hobday AJ (2006) Automated acoustic tracking of aquatic

animals: scales, design and deployment of listening station arrays. Mar Freshw Res 57:1–13.

How JR, de Lestang S (2012) Acoustic tracking: issues affecting design, analysis and interpretation of data from movement studies. Mar Freshw Res 63:312–324.

Huveneers C, Simpfendorfer CA, Kim S, Semmens JM, Hobday AJ, Pederson H, Stieglitz T, Vallee R, Webber D, Heupel MR (2016) The influence of environmental parameters on the performance and detection range of acoustic receivers. Methods Ecol Evol 7:825–835.

Mathies NH, Ogburn MB, McFall G, Fangman S (2014) Environmental interference factors affecting detection range in acoustic telemetry studies using fixed receiver arrays. Mar Ecol Prog Ser 495:27–38.

Medwin H, Clay CS (1997) Fundamentals of acoustical oceanography. Academic press, New York City, New York, pp. 712.

Payne NL, Gillanders BM, Webber DM, Semmens JM (2010) Interpreting diel activity patterns from acoustic telemetry: the need for controls. Mar Ecol Prog Ser 419:295–301.

Radford CA, Jeffs AG, Tindle CT, Montgomery JC (2008) Temporal patterns in ambient noise of biological origin from a shallow water temperate reef. Oecologia 156:921–929.

Simpfendorfer CA, Heupel MR, Collins AB (2008) Variation in the performance of acoustic receivers and its implication for positioning algorithms in a riverine setting. Can J Fish Aquat Sci 65:482–492.

Singh L, Downey NJ, Roberts MJ, Webber DM, Smale MJ, Van den Berg MA, Harding RT, Engelbrecht DC, Blows BM (2009) Design and calibration of an acoustic telemetry system subject to upwelling events. African J Mar Sci 31:355–364.

Voegeli FA, Pincock DG (1996) Overview of underwater acoustics as it applies to telemetry. In: *Underwater Biotelemetry*. Baras E, Philippart JC (eds) Liege: University of Liege, p 22-30.

Winter JD (1996) Advances in underwater biotelemetry. Fish Tech:555–590.

Winton M V, Kneebone J, Zemeckis DR, Fay G (2018) A spatial point process model to estimate individual centres of activity from passive acoustic telemetry data. Methods Ecol Evol 9:2262–2272.

Table S2. Characteristics of range tests conducted at five locations along the coast of New South Wales.

Receiver location	Start date	End date	Duration (d)	Distances measured (m)	Additional distance measurements (m) [time frame]
Evans Head	2019-07-15	2019-11-30	138	100, 200	500 [2019-11-27 to 2019-11-30]
South West Rocks	2019-07-15	2019-11-30	136	100, 200	500 [2019-11-20 to 2019-11-30]
Port Macquarie	2019-07-22	2019-11-30	132	100, 200	500 [2019-10-23 to 2019-11-30]
Forster	2019-07-18	2019-11-30	136	100, 200	NA
Hawks Nest	2019-07-22	2019-11-30	132	100, 200	500 [2019-11-04 to 2019-11-30]

Table S3. Model selection summaries for range test detection data. For each model, all combinations were run and ranked based on their parsimony; the five best models are shown.

Model	LogLik	AICc	ΔAICc	Weight	Deviance
All variables	-62125.27	124284.1	0.00	1	21.54%
All variables except *Lunar phase*	-62248.50	124526.8	242.65	0	21.32%
All variables except *Time of day*	-62407.01	124843.7	559.59	0	21.03%
All variables except *Tide*	-62475.32	124982.2	698.02	0	20.91%
All variables except *Lunar phase* and *Time of day*	-62529.30	125088.1	803.93	0	20.81%
Null model (presence ~ distance + location)					13.19%

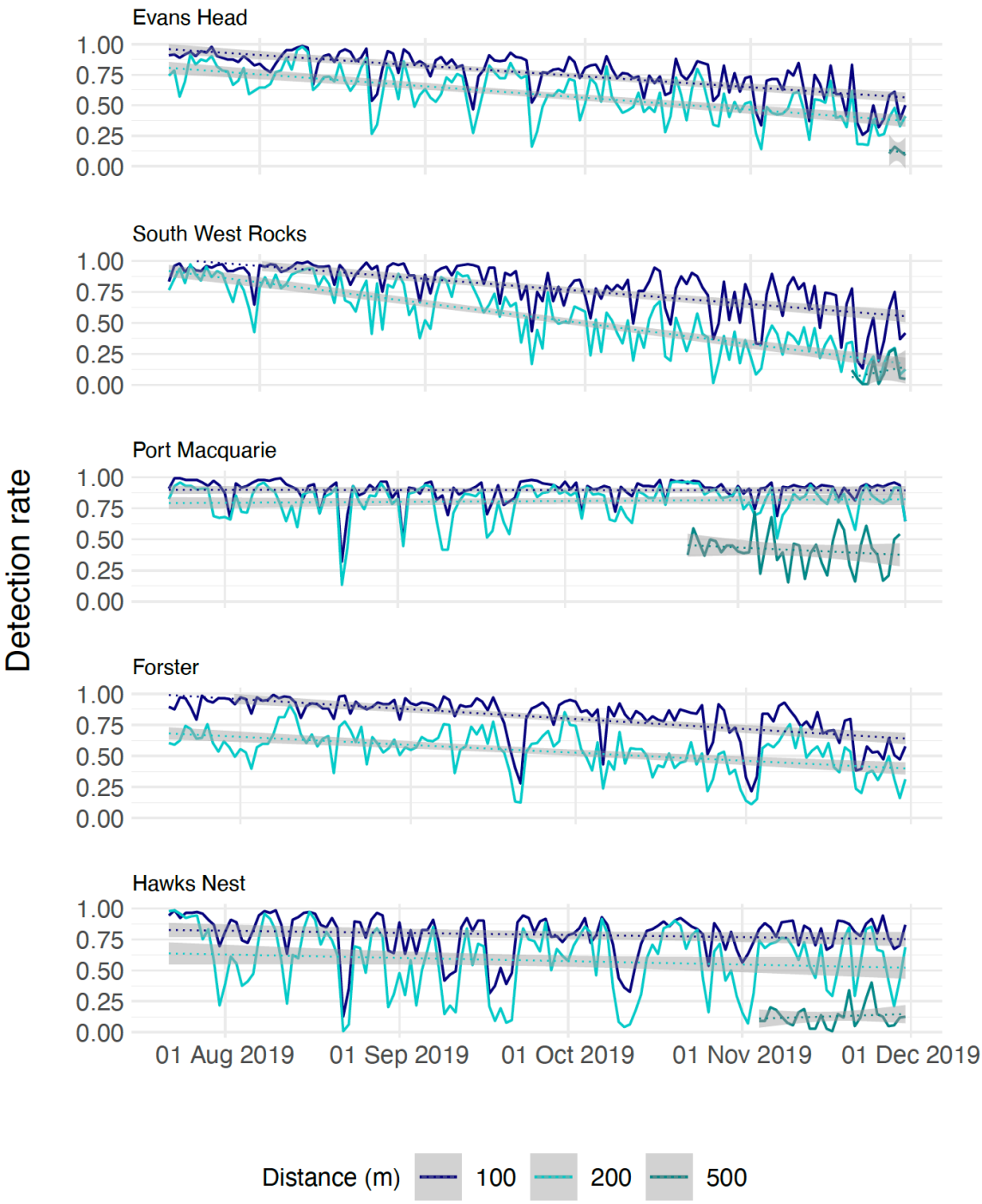

Figure S1. Daily detection rates of range test tags at 100m, 200m and 500m over the range test period (see Table S2 for receiver specific range test start dates). Grey shading indicates 95 % confidence limits.

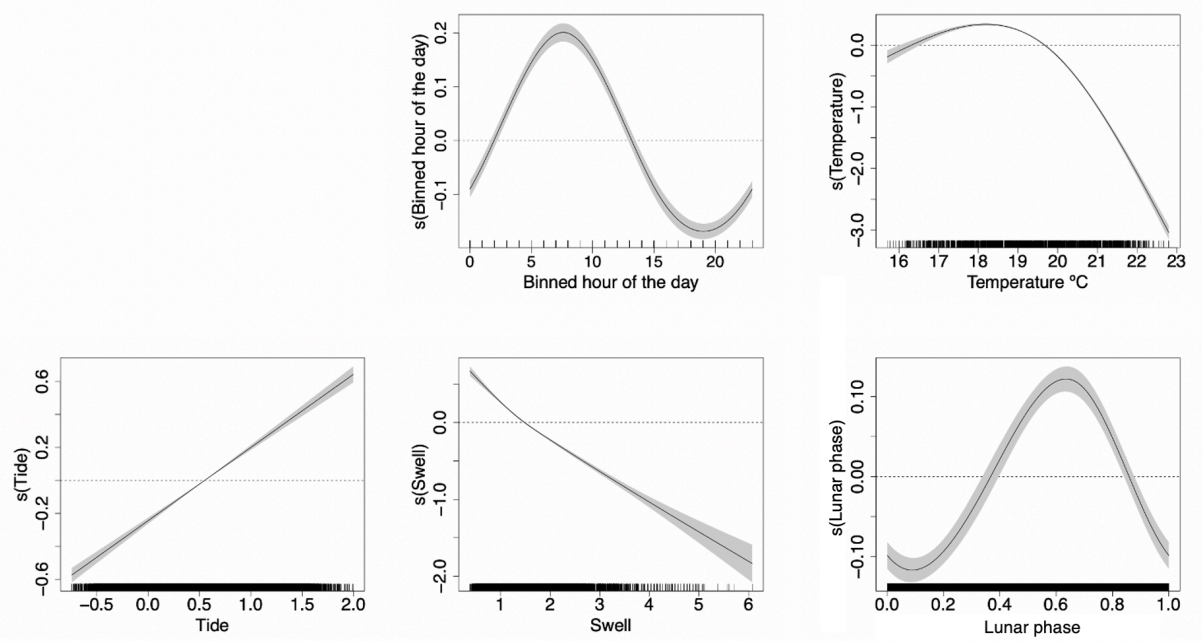

Figure S2. Response curves of the variables included in the most supported model explaining range test detections across receivers at Evans Head, South West Rocks, Port Macquarie, Forster and Hawks Nest, across both distances tested (i.e. 100 m and 200 m). Grey shading indicates 95% confidence limits. Zero on the vertical axes corresponds to no effect of the explanatory variable. Lunar phase values correspond to new moon (0), first quarter (0.25), full moon (0.5) and second quarter (0.75).

Table S4. Results of the generalized additive model constructed to assess the influence of environmental variables on the detection rate of fixed delay transmitters (V16-6L, InnovaSea), deployed at 100 m and 200 m distance to receiver locations at Evans Head, South West Rocks, Port Macquarie, Forster and Hawks Nest. % DE: percent of unique deviance explained by each variable tested.

Predictor added to model	df	$p(X^2)$	% DE
Time of day	1.988	< 0.001	0.51
Water temperature	2.969	< 0.001	5.14
Tidal height	1.002	< 0.001	0.63
Swell height	2.864	< 0.001	2.05
Lunar phase	1.974	< 0.001	0.22
Location			4.90
Distance			8.49
Full model			21.54
Null model (presence~ distance+ location)			13.19

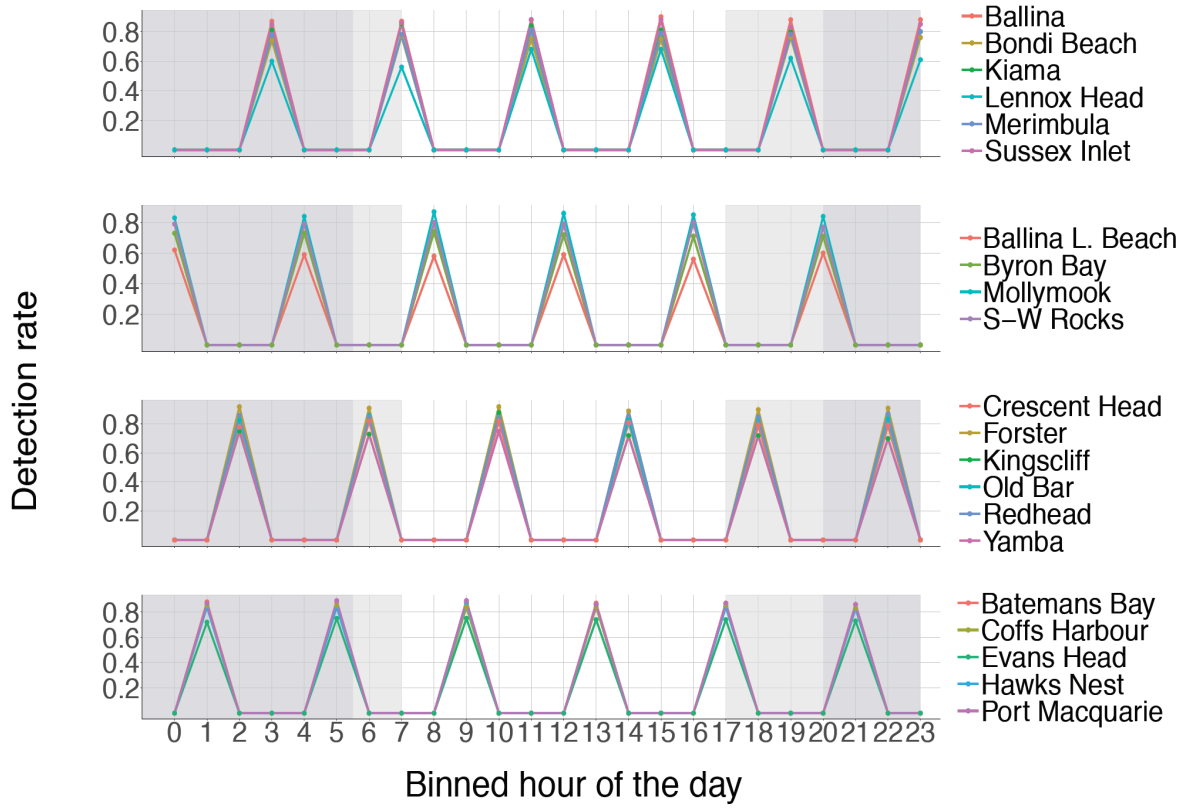

Figure S3. Detection rates of sentinel tags by VR4G receivers, pooled by hourly bin between 01 December 2016 - 30 November 2018. Areas shaded in grey indicate approximate night time.

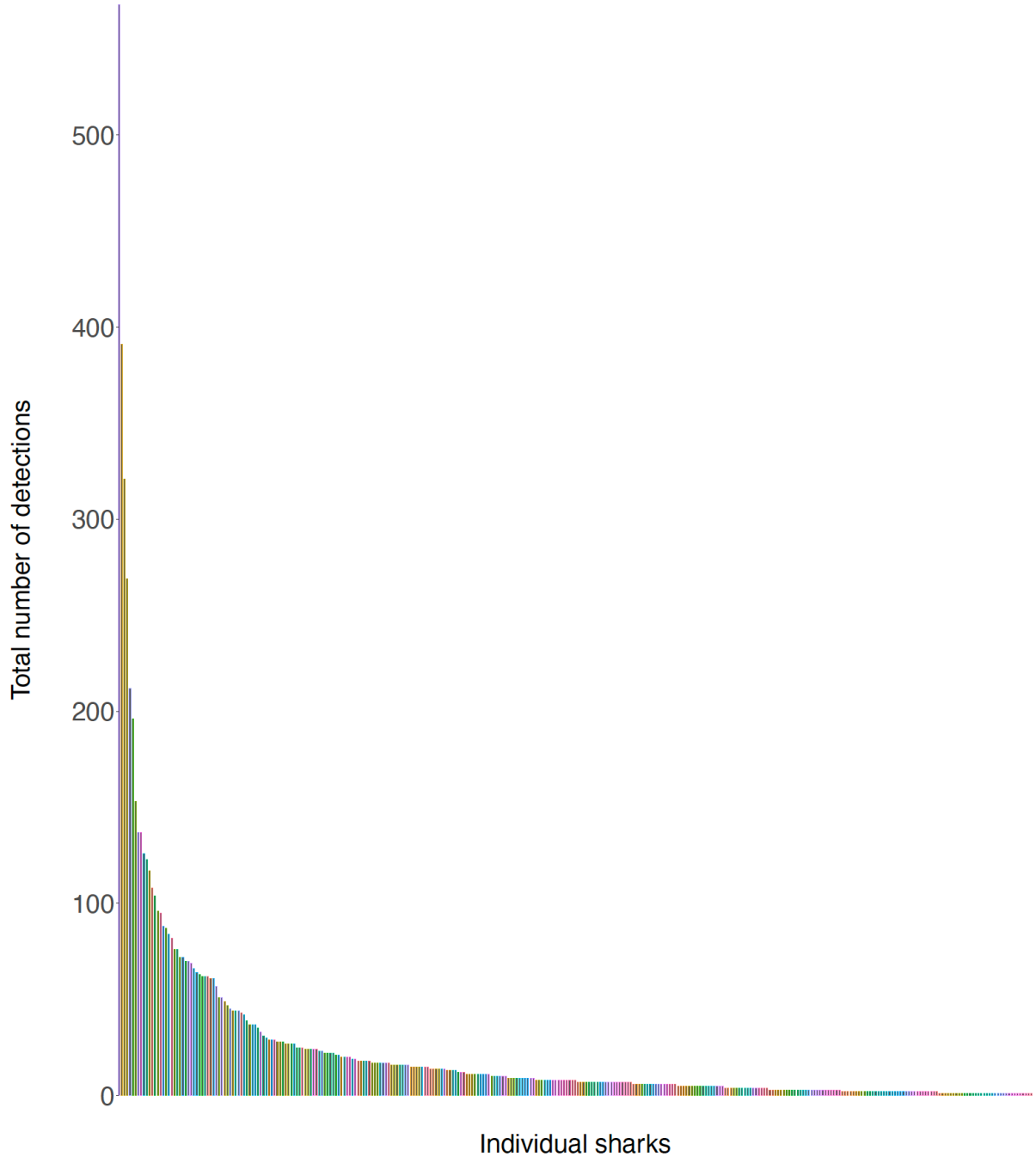

Figure S4. Total number of detections (after hourly binning) for all sharks across all receiver locations (except for Ballina Lighthouse and Lennox Head, which were excluded from all analyses) between 1 December 2016 and 30 November 2019. Each coloured bar represents one individual. The first ten individuals together account for one third of the total detections.

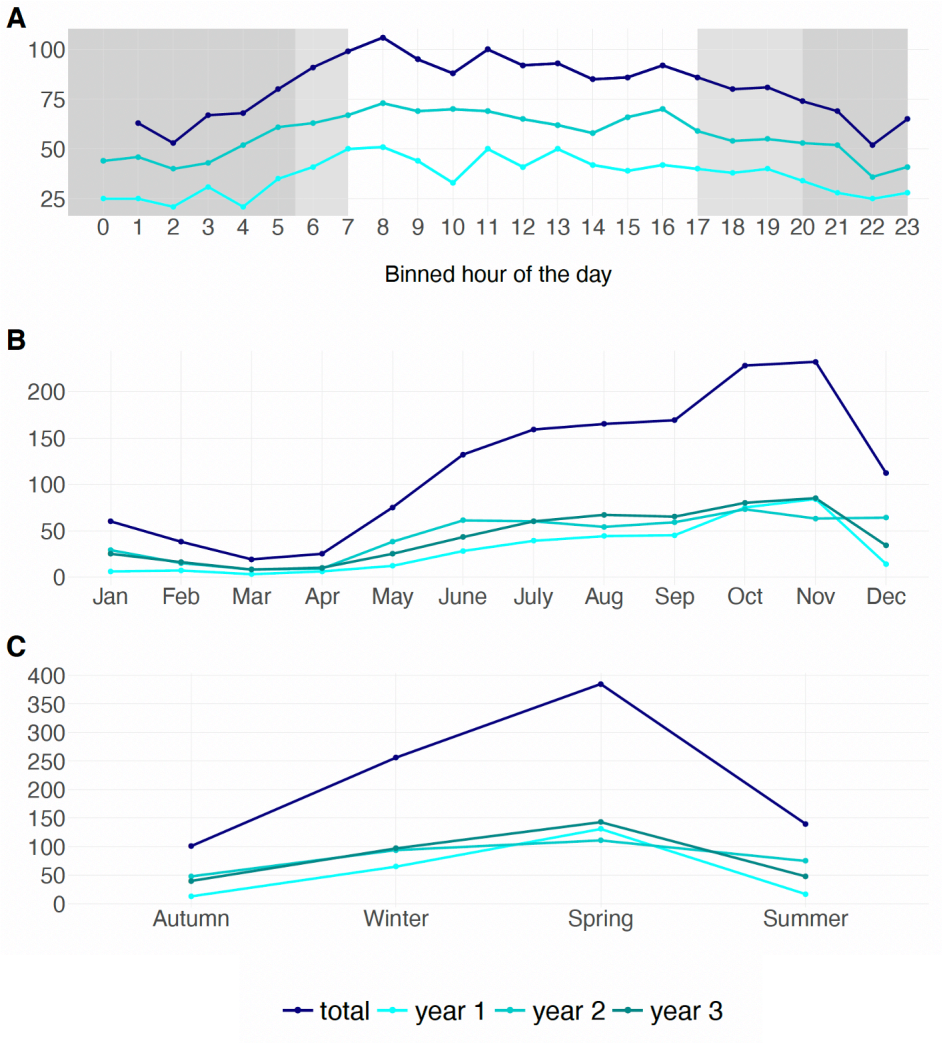

Figure S5. Total number of A) individual sharks detected per time of day (binned time data: 0 = 00:00 h – 00:59 h…23 = 23:00 h – 23:59 h); B) month; and C) season across all receiver locations between 1 December 2016 and 30 November 2019. Areas shaded in grey indicate approximate night-time.

Table S5. Generalized additive model selection summaries for i) the full dataset, including all tagged individuals; ii) a partial dataset, excluding the ten most detected individuals. For each model, all combinations were run and ranked based on their parsimony. The five best models are shown. Null models including only ID and location variables are shown for comparison.

Model	LogLik	AICc	ΔAICc	Weight	Deviance	AUC
Full dataset						
All variables	-29465.12	59650.7	0.00	0.919	20.95%	0.87
All variables except *Tidal height*	-29470.10	59655.6	4.85	0.000	20.90%	0.87
All variables except *Lunar phase*	-29477.27	59671.9	21.14	0.000	20.91%	0.87
All variables except *Tidal height* and *Lunar phase*	-29482.19	59676.8	26.03	0.000	20.90%	0.87
All variables except *Water temperature*	-29513.05	59740.5	89.77	0.000	20.82%	0.87
Null model (presence ~ ID + location)	-30124.46	60943.5	1292.82	0.000	19.18%	0.86
Dataset excluding 10 most detected sharks						
All variables	-20743.65	42183.3	0.00	0.930	17.00%	0.84
All variables except *Tidal height*	-20747.34	42188.5	5.17	0.007	16.94%	0.84
All variables except *Lunar phase*	-20756.25	42204.5	21.21	0.000	16.90%	0.84
All variables except *Tidal height* and *Lunar phase*	-20759.74	42209.5	26.23	0.000	16.89%	0.84
All variables except *Water temperature*	-20785.05	42260.7	77.39	0.000	16.79%	0.84
Null model (presence ~ ID + location)	-21263.69	43202.3	1018.96	0.000	14.90%	0.82

Table S6. Results of the generalized additive model constructed to assess the influence of environmental and temporal variables on the occurrence of acoustically tagged white sharks along the coast of New South Wales, Australia. %DE: percent of unique deviance explained by each variable tested.

Predictor added to model	df	$p(X^2)$	%DE
Month	1.99	< 0.001	0.57
Time of day	1.99	< 0.001	0.46
Water temperature	2.80	< 0.001	0.09
Tidal height	2.54	< 0.01	0.01
Swell height	1.64	< 0.001	0.27
Lunar phase	1.95	< 0.001	0.03
Shark ID			0.16
Location			17.26
Full model			20.95
Null model (presence~ID+ location)			19.18

Table S7. Sensitivity test results of generalized additive models based on five datasets containing the same presences but different absences. %DE: percent of deviance explained by the full model of each dataset.

	Set 1		Set 2		Set 3		Set 4		Set 5	
Predictor added to model	df	$p(X^2)$	df	$p(X^2)$	df	$p(X^2)$	df	$p(X^2)$	df	$p(X^2)$
Month	1.99	< 0.001	1.92	< 0.001	1.98	< 0.001	1.99	< 0.001	1.98	< 0.001
Time of day	1.99	< 0.001	1.98	< 0.001	1.98	< 0.001	1.99	< 0.001	1.99	< 0.001
Water temperature	2.80	< 0.001	2.69	< 0.001	2.78	< 0.001	2.73	< 0.001	2.82	< 0.001
Tidal height	2.54	< 0.01	2.51	< 0.01	2.70	< 0.01	2.69	< 0.05	2.96	< 0.05
Swell height	1.64	< 0.001	1.06	< 0.001	1.70	< 0.001	1.83	< 0.001	1.83	< 0.001
Lunar phase	1.95	< 0.001	1.93	< 0.001	1.96	< 0.001	1.80	< 0.001	1.80	< 0.001
Full model %DE	20.95		21.00		20.9		21.1		21.1	

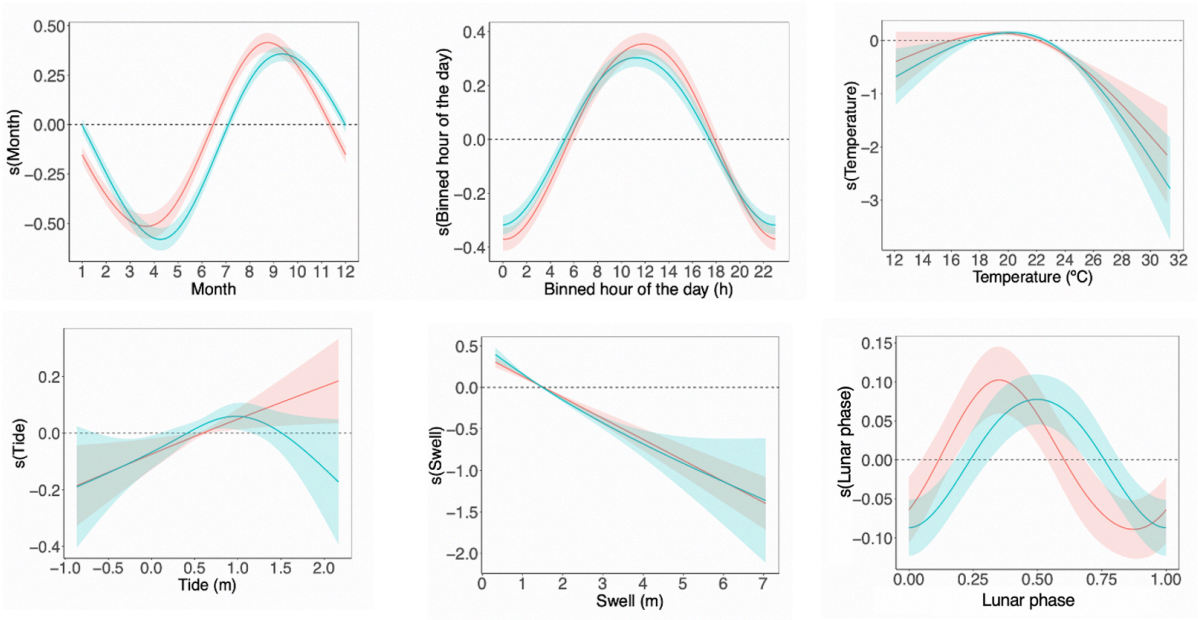

Figure S6. Comparison of generalized additive model response curves between the full dataset (blue) and a subset, excluding the 10 most detected sharks (red). Grey shading indicates 95 % confidence limits. Zero on the vertical axes corresponds to no effect of the explanatory variable. Lunar phase values correspond to new moon (0), first quarter (0.25), full moon (0.5) and second quarter (0.75).

Table S8. Summaries of the most supported models (by life stage) for predicting white shark occurrence along the coast of New South Wales, Australia. Models were run separately for each group i) young-of-the-year-sharks (n = 24); ii) sub-adult sharks (n = 33); iii) a subset of juvenile sharks (n = 15), iiii) juvenile sharks (n = 387). For each model, all combinations were run and ranked based on their parsimony. Only the top model is shown for each group. %DE: percent of full deviance explained by the top model for each group.

Model	LogLik	AICc	ΔAICc	Weight	%DE
Young-of-the-year					
All variables except *Tide*	-680.397	1435.1	0.00	0.436	41.7
Sub-adults					
Month + Time of day	-817.701	1734.3	0.00	0.220	26.5
Juvenile subset					
Month + Time of day + Swell height	-981.949	2047.9	0.00	0.364	27.2
Juveniles					
All variables	-29473.32	55222.64	0.00	0.916	21.2

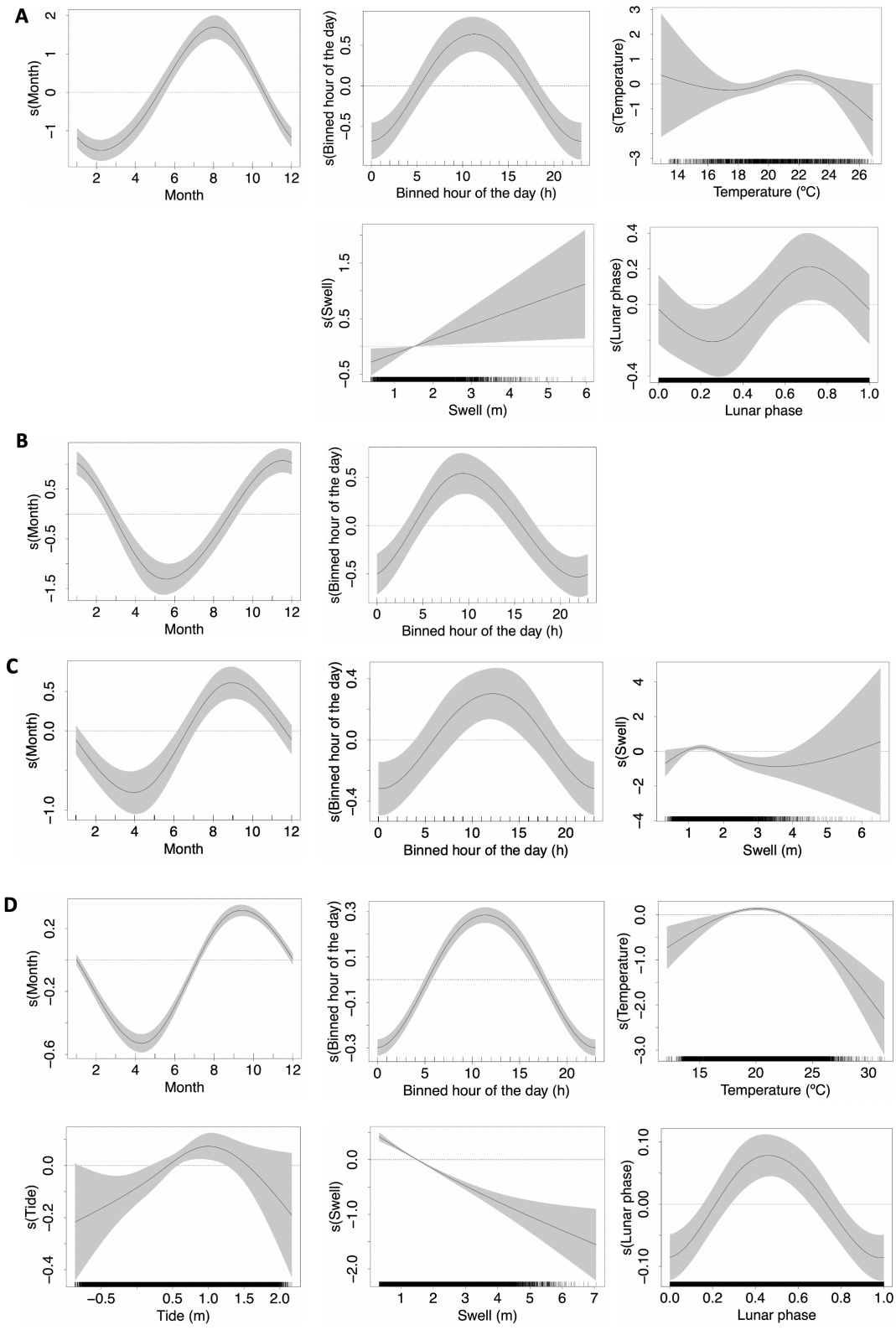

Figure S7. Response curves of the variables included in the most supported models for predicting white shark occurrence along the coast of New South Wales, Australia, grouped by life stage (see Table S8). (A) young-of-the-year sharks. (B) sub-adult sharks. (C) a subset of juvenile sharks (n=15). (D) juvenile sharks (total). Grey shading indicates 95% confidence limits. Positive values on the vertical axes indicate an increase probability of occurrence, while negative values indicate an increased probability of absence. Lunar phase values correspond to new moon (0), first quarter (0.25), full moon (0.5) and second quarter (0.75).

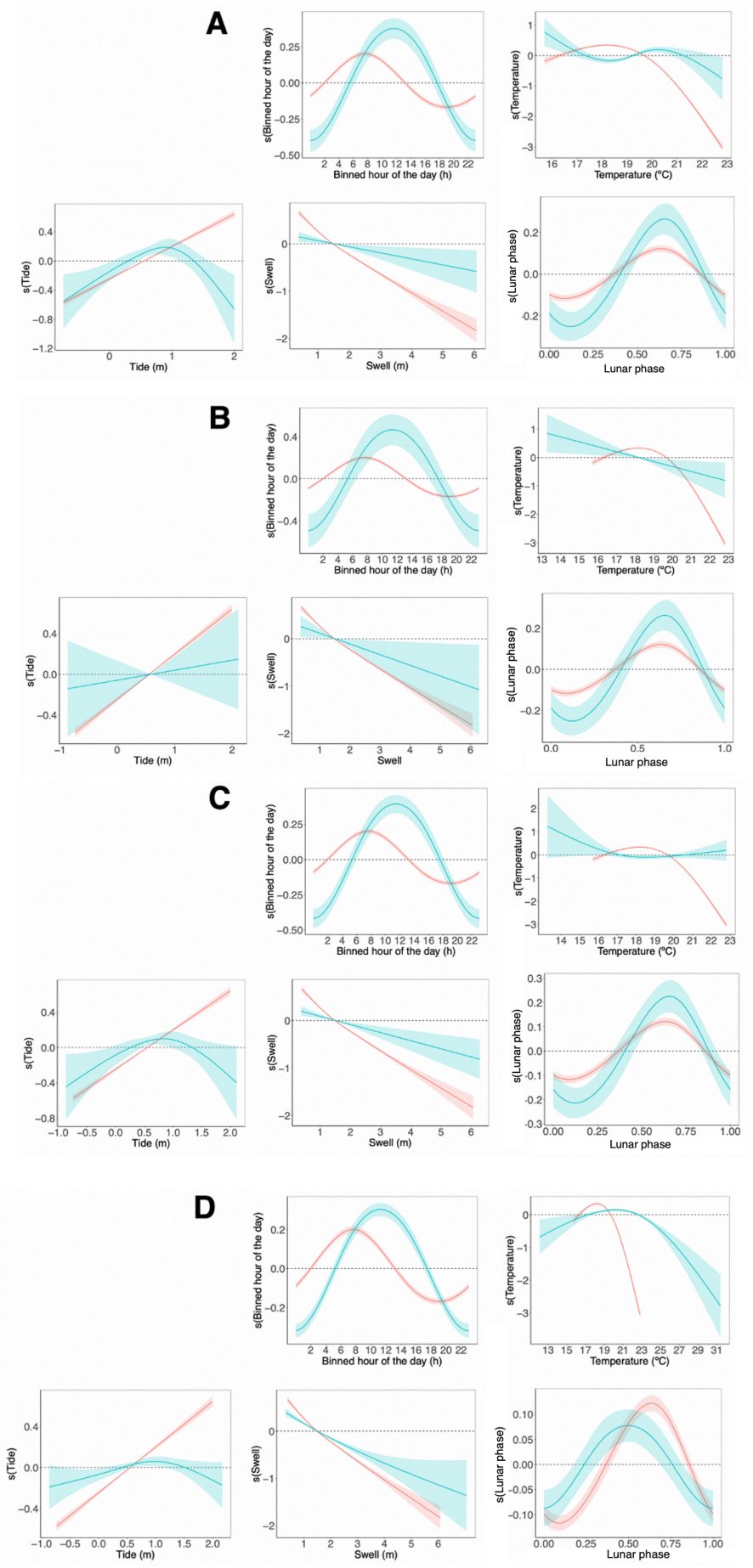

Figure S8. Comparison of Generalised additive model (GAM) response curves between range test and white shark detection data. Response curves of range test detection data across all range test locations and distances are indicated in red across A), B), C) and D). Blue indicates GAM response curves of (A) white shark presences during the range test period at range test receiver locations only; (B) white shark presences during the range test period at non-range test receiver locations only; (C) white shark presences during the range test period across all receiver locations; (D) white shark presences across the 3-year study period across all 19 receiver locations. Shading indicates 95% confidence limits. Zero on the vertical axes corresponds to 'no effect' of the explanatory variable. Lunar phase values correspond to new moon (0), first quarter (0.25), full moon (0.5) and second quarter (0.75).

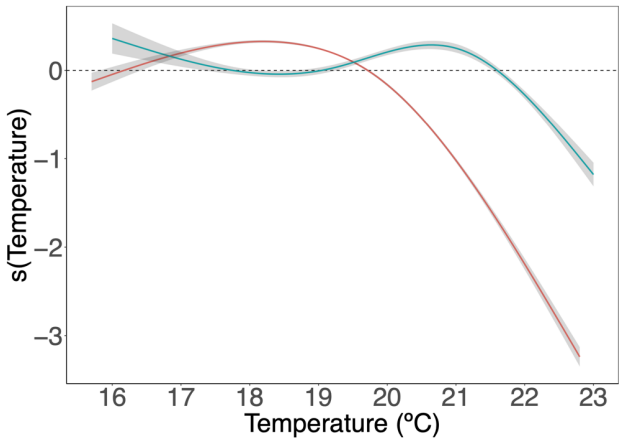

Figure S9. GAM response curves for white shark occurrences across the three-year study period across all 19 receiver locations (blue) and range test detections (red) covering the temperature range observed during the range test period only. Grey shading indicates 95% confidence limits. Zero on the vertical axes corresponds to no effect of the explanatory variable.